Bonse-Hart Angular Profiles Realized for Multiply Bragg Reflected Neutrons

Apoorva G. Wagh* and Veer Chand Rakhecha*
Solid State Physics Division, Bhabha Atomic Research Centre, Mumbai 400085, India

Wolfgang Treimer
University of Applied Sciences (TFH) Berlin, Fachbereich II, Luxemburger Strasse 10 D-13353 Berlin and Hahn-Meitner-Institut Berlin, SF1, D-14109 Berlin, Germany

(Received 22 May 2001; published 30 August 2001)

We have produced a monochromatic neutron beam with the sharpest angular profile to date. Multiple Bragg reflections from optimally designed channel-cut silicon single crystals have produced neutron beams with theoretical Darwin angular profiles. This experiment constitutes the first realization of the proposal made by Bonse and Hart 35 years ago and opens up avenues for ultrasmall angle neutron scattering studies down to wave vector transfers of 10^{-5} Å^{-1}.

DOI: 10.1103/PhysRevLett.87.125504 PACS numbers: 61.12.Bt, 03.75.Be, 61.12.Ex

Experimenters yearn for a highly parallel monochromatic beam. For instance, ultra-small angle neutron (or x-ray) scattering (USANS/USAXS) studies [1] of momentum transfers $Q \sim 10^{-5} - 10^{-3}$ Å^{-1}, to characterize samples [2] containing agglomerates of dimensions 10^4 Å, require an incident beam collimation of a few arc sec. Bonse and Hart [3] proposed a number (n) of successive identical Bragg reflections from two slabs of a channel-cut monolithic single crystal to achieve such a high collimation. The tails of the multiply reflected intensity fraction R^n get trimmed preferentially compared to the peak (equal to unity), R denoting the reflectivity for each Bragg reflection. This happens since the smaller a positive fraction, the faster it reduces when raised to a positive integer n. Such a beam thus has a nearly rectangular angular profile, a few arc sec wide. However, the observed tail intensities of such multiply Bragg reflected x-ray [3,4] and neutron [5–7] beams have been a few orders of magnitude higher than so expected.

A plausible explanation for these excessive tail intensities was offered [8] in terms of dynamical diffraction effects undergone by neutrons (and x rays) incident outside the total reflectivity regime. According to the dynamical diffraction theory [8–11], the incident and diffracted waves of a Bragg reflection are coupled coherently together and traverse the perfect crystal as a single entity. Figure 1 depicts a Bragg reflection from a perfect crystal slab, with an asymmetry factor, $\gamma_r = -\sin(\theta_B + \theta_S)/\sin(\theta_B - \theta_S)$, where θ_B and θ_S stand for the Bragg angle and the angle between the Bragg planes and the front face, respectively. Neutrons incident along a ray **I** get reflected along the ray **D** at the front face. The corresponding reflectivity is given by the Darwin expression

$$\begin{aligned} R_D &= 1, \qquad |y| \le 1, \\ &= (|y| - \sqrt{y^2 - 1})^2, \qquad |y| > 1, \end{aligned} \tag{1}$$

as a function of the reduced incidence angle y [8–11]. Over the total reflectivity range ($|y| \le 1$), all the incident neutrons are reflected along **D**. At each angle of incidence outside this range, a pair of tie points on the α (or β) branch of the dispersion surface gets selected by boundary conditions. At the front face, however, only one of these tie points, dictating propagation of the unreflected fraction, $1 - R_D$, of neutrons *into* the crystal, gets excited. If these neutrons reach the back face, they excite the other tie point there. As $|y|$ increases, this neutron propagation occurs at progressively larger angles to the front face (Fig. 1). In the limit of incidence well off the Bragg condition, the direction of neutron propagation approaches the incident beam direction. These neutrons subsequently diffract at the side, back, and front faces of the slab. A fraction of these

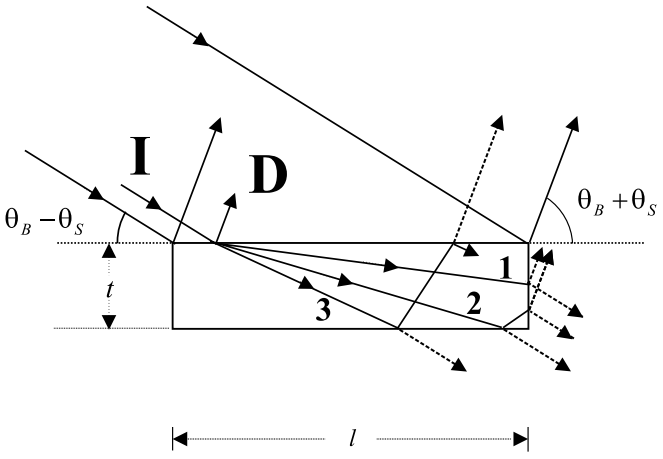

FIG. 1. Asymmetric Bragg reflection of a neutron beam incident on a perfect crystal slab (schematic). Within the total reflectivity regime (spanning a few arc sec), neutrons incident along a representative ray **I** get fully reflected along the ray **D**. As neutron incidence deviates from this regime, the fraction of neutrons not reflected along **D** propagates into the crystal successively along rays labeled **1**, **2**, and **3**. Some of these neutrons exit the side, back, and front faces as stray beams (shown by dashed rays).

 0031-9007/01/87(12)/125504(4)$15.00

neutrons emanates from the three faces (dashed rays in Fig. 1) and propagates with the multiply Darwin reflected beam, without suffering further reflection and hence attenuation. Such dynamical diffraction effects have indeed been observed for x rays [12–14] and neutrons [15,16]. These effects can account for the observed spurious tails of the genuine multiply reflected beam.

The stray beams shown by dashed rays in Fig. 1 ought to be eliminated to obtain a clean Darwin reflection. Stray beams emanating from the side and back faces can be purged by covering these faces with a neutron absorbing material. The stray beam exiting the front face, however, is inseparable from the genuine Darwin reflected beam. It is therefore necessary not to allow the beams reflected at the back face to reach the front face. This can be accomplished by *increasing* the slab thickness t until

$$t > t_m = \frac{l \tan\theta_B}{2}\left[1 - \frac{\sin^2\theta_S}{\sin^2\theta_B}\right]. \qquad (2)$$

l denoting the length of the crystal slab (Fig. 1). Such an optimally thick perfect crystal slab will produce a clean Darwin reflection when its side and back faces are covered with an absorber. This design ensures that none of the neutrons propagating into the slab can reemerge into the genuine Bragg reflected beam. The beam so reflected can be Darwin reflected back in the incident direction by an identical slab of opposite asymmetry factor γ_r^{-1}. Hence n such optimal slab modules located alternately on opposite sides of the channel in a monolithic channel-cut crystal (see inset in Fig. 4), will yield the theoretical multiple Darwin reflected profile R_D^n. These considerations apply to multiple Bragg reflections of x rays [3,4] as well, albeit to a smaller extent due to their stronger absorption within crystals.

For a slab of nonoptimal geometry, however, contamination by the stray beams (see Fig. 1) produces a reflectivity approaching the Ewald expression, viz.

$$\begin{aligned} R_E &= 1, \qquad |y| \le 1, \\ &= 1 - \sqrt{1 - y^{-2}}, \qquad |y| > 1. \end{aligned} \qquad (3)$$

For a given reflection, the Ewald reflectivity (3) is about twice as great as the Darwin reflectivity (1) in the tail region ($|y| > 3$).

Extensive efforts at several laboratories [3–7] the world over for the past three and a half decades to realize the Bonse-Hart proposal, have not succeeded in attaining even the Ewald angular profiles. In contrast, we have achieved here the ideal Darwin angular profile for a multiple symmetric Bragg reflection, using an optimally designed channel-cut silicon crystal.

The experiment was carried out [17,18] at the V12b Double Crystal Diffractometer setup in the Berlin Neutron Scattering Center (BENSC) of the Hahn-Meitner-Institut, Germany. The setup comprises a premonochromator, monochromator and analyzer operating in the $(+,-,+)$, i.e., nondispersive, configuration. In the first run, a neutron beam with a mean wavelength $\lambda_0 = 5.229$ Å from a pyrolitic graphite premonochromator illuminated an asymmetric single crystal silicon monochromator. The monochromator crystal surface was cut at $\theta_S = 26.8°$ to the {111} planes, corresponding to the asymmetry factor $\gamma_r = -2.005$. An optimally designed channel-cut silicon crystal placed at the analyzer position, produced a triple symmetric {111} Bragg reflection of the 10 mm wide and 20 mm high neutron beam. The rocking curve of the channel-cut crystal recorded in this configuration is presented in Fig. 2. The convolution of the single asymmetric Ewald reflectivity R_{Ea} with the triple symmetric Darwin reflectivity R_{Ds}^3, computed with the appropriate Debye-Waller factor [15] and a Gaussian wavelength distribution ($\sigma_\lambda = \lambda_0/100$) of the neutron beam, is also shown for comparison. The experimental rocking curve is in excellent agreement with the theoretical prediction over the entire scan spanning over 4 orders of magnitude in intensity.

Next, installing this optimal channel-cut triple reflector at the monochromator position and a conventional (nonoptimal) channel-cut triple symmetric reflector at the analyzer position, we recorded triple-triple {111} rocking curves (Fig. 3). The data (circles) agree with the theoretical curve (triangles) comprising a convolution of the triple symmetric Darwin (R_{Ds}^3) and triple symmetric Ewald (R_{Es}^3) reflectivities.

Finally, we replaced the nonoptimal reflector analyzer with another optimal triple symmetric Bragg reflector. The corresponding rocking curve is shown in Fig. 4. The data (circles) agree with the theoretical curve (triangles) for Darwin reflections $R_{Ds}^3 \star R_{Ds}^3$, over an intensity range spanning 5 orders of magnitude. The spurious tails have

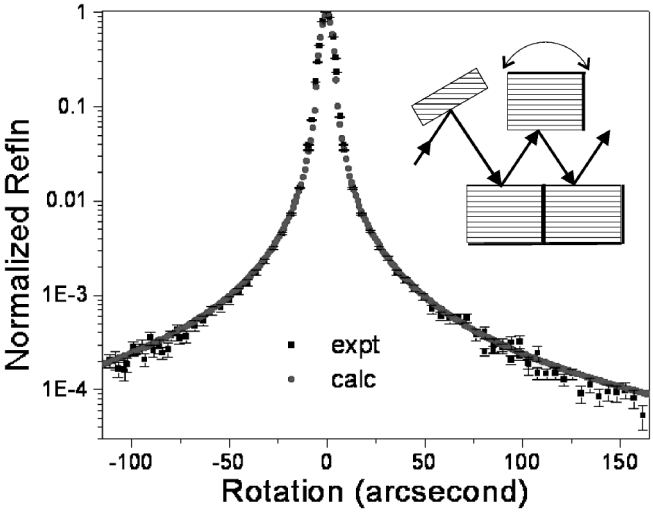

FIG. 2. Rocking curve between a single asymmetric and a triple symmetric, {111} Bragg reflections of 5.229 Å neutrons from perfect silicon crystals. The experimental data (squares) agree with theory (circles).

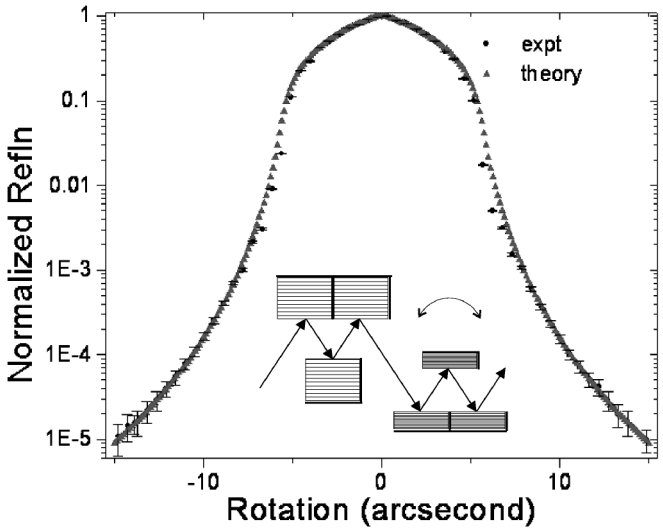

FIG. 3. Rocking curve between an optimal triple symmetric and a nonoptimal triple symmetric {111} Bragg reflection from channel-cut silicon single crystals. Circles represent the experimental points, and triangles the calculated triple Darwin-triple Ewald convoluted angular profile.

been eliminated completely. This constitutes the first realization of the proposal made by Bonse and Hart [3] over 35 years ago. The best previous Bonse-Hart profile [6], recorded for quadruple-triple symmetric Bragg reflections at the USANS setup in ORNL, is also shown (inverted triangles) in the figure. The present results thus mark well over an order of magnitude improvement over all Bonse-Hart multiple Bragg reflection profiles reported previously.

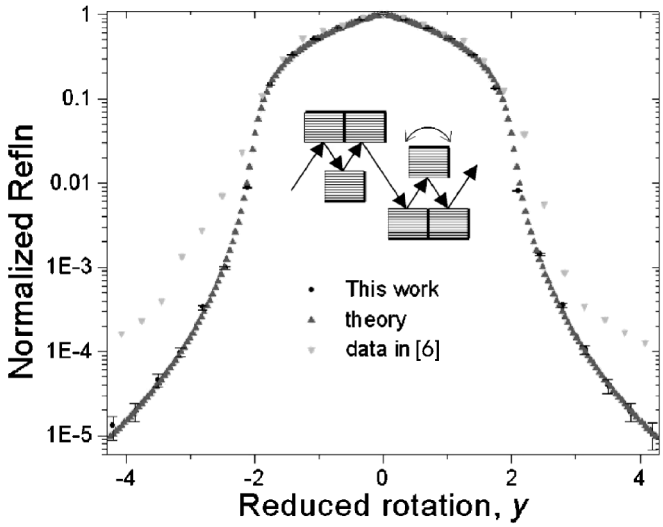

FIG. 4. Rocking curve between two optimal triple symmetric {111} Bragg reflections from channel-cut silicon single crystals. The experimental data (circles) agree closely with the calculated triple-triple Darwin profile (triangles) and mark an order of magnitude improvement over the previous best quadruple-triple symmetric {111} Bragg reflection profile (inverted triangles) reported in Ref. [6].

Each of our triple Bragg reflecting channel-cut crystals thus produces the theoretical triple Darwin reflectivity.

In contrast, none of the previously reported channel-cut crystals [3–7] has succeeded in achieving even the inferior Ewald reflectivity [see Eqs. (1) and (3)], expected due to their nonoptimal geometries, for x-ray and neutron beams. Their observed excessive tail intensities were conjectured to arise from thermal diffuse scattering [19] within the volume of the silicon *perfect* crystals. The tail-free Darwin angular profile (Fig. 4) achieved in the present experiment with thicker slabs (and hence larger crystal volumes) however, rules out the possibility of thermal diffuse scattering making a significant contribution to the spurious tails [3–7]. The tails may have two plausible explanations. Neutrons (or x rays) propagating into the reflector slabs and exiting their side and back faces [see Fig. 3(a) in [8], Fig. 1 in [17], and Fig. 1 above] may copropagate and contaminate the multiply reflected beam [3–7]. Diffraction at slits and edges encountered between the first and the second channel-cut crystals can be another possible source of the observed spurious tails. Any macroscopic (cm size) slit or absorber edge introduced to sharpen the beam profile can in actuality broaden it by scattering neutrons (or x rays) through such small angles. The corresponding rocking curve would hence represent a USANS/USAXS spectrum with the slit or edge serving as a "sample."

Figure 5 illustrates this diffraction effect with a pair of spectra recorded with and without a 10 mm wide cadmium slit at the sample position. The slit enhances the intensity in the tail region by an order of magnitude. Scattering events with momentum transfers down to 3.7×10^{-5} Å^{-1} are clearly discerned. Fraunhofer broadening of the sharp central peak in the angular profile of neutrons triple Laue reflected from a perfect silicon crystal, on passage through 2.5 and 5 mm wide slits has been observed [20] earlier.

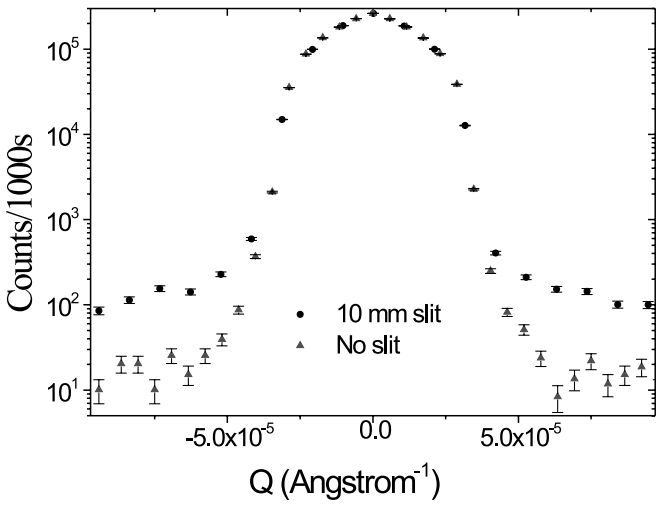

FIG. 5. Diffraction at a slit placed between the two optimal triple reflecting channel-cut crystals. Rocking curves recorded with (circles) and without (triangles) a 10 mm wide cadmium slit sample demonstrate the USANS capability of our setup.

The present experiment has observed the slit diffraction effect in the tail region. An extensive series of further experiments [21] with slits as well as edges on the left or right side of the beam, has led to a complete delineation of these neutron diffraction phenomena. The Darwin profiles attained at our setup [18] can extend the background-free USANS measurement capability to wave vector transfers $Q \sim 10^{-5}$ Å^{-1}.

To recapitulate, a tail-free Darwin angular profile has been obtained for the first time for a multiply Bragg reflected beam. The monochromatic neutron beam produced in the present work has the sharpest angular profile reported to date. The Bonse-Hart proposal, made more than 35 years earlier, has thus been implemented in its totality. This work opens up new possibilities for SUSANS (super-ultra-small-angle neutron scattering) studies.

We wish to thank Th. Wilpert, M. Strobl, and A. Hilger for experimental assistance. One of us (A. G. W.) acknowledges local hospitality received from BENSC, HMI during the experimental runs. This work was partly supported by the EU project PECNO.

*Electronic address: nintsspd@magnum.barc.ernet.in

[1] *Proceedings of XIth International Conference on Small-Angle Scattering (SAS99), Brookhaven, 1999,* edited by D. K. Schneider and S.-H. Chen [J. Appl. Cryst. **33**, 421–868 (2000)].
[2] See, for instance, P.-G. deGennes, *Scaling Concepts in Polymer Physics* (Cornell University Press, Ithaca, 1979).
[3] U. Bonse and M. Hart, Appl. Phys. Lett. **7**, 238 (1965).
[4] T. Koga, M. Hart, and T. Hashimoto, J. Appl. Cryst. **29**, 318 (1996).
[5] D. Schwahn, A. Miksovsky, H. Rauch, E. Seidl, and G. Zugarek, Nucl. Instrum. Methods Phys. Res., Sect. A **239**, 229 (1985).
[6] M. Agamalian, D. K. Christen, A. R. Drews, C. J. Glinka, H. Matsuoka, and G. D. Wignall, J. Appl. Cryst **31**, 235 (1998).
[7] G. Kroupa, G. Bruckner, O. Bolik, M. Zawisky, M. Hainbuchner, G. Badurek, R. J. Buchelt, A. Schricker, and H. Rauch, Nucl. Instrum. Methods Phys. Res., Sect. A **440**, 604 (2000).
[8] A. G. Wagh, Phys. Lett. A **121**, 45 (1987); **123**, 499 (1987).
[9] W. H. Zachariasen, *Theory of X-Ray Diffraction in Crystals* (Wiley, New York, 1963).
[10] B. W. Batterman and H. Cole, Rev. Mod. Phys. **36**, 681 (1964).
[11] A. G. Wagh and V. C. Rakhecha, Prog. Part. Nucl. Phys. **37**, 485 (1996).
[12] G. Borrmann, G. Hildebrandt, and H. Wagner, Z. Phys. **142**, 406 (1955).
[13] A. J. Authier, Phys. Radium **23**, 961 (1962).
[14] A. G. Wagh (unpublished).
[15] C. G. Shull, J. Appl. Cryst. **6**, 257 (1973).
[16] A. Zeilinger, C. G. Shull, J. Arthur, and M. A. Horne, Phys. Rev. A **28**, 487 (1983).
[17] A. G. Wagh, V. C. Rakhecha, and W. Treimer, *BENSC Experimental Reports 1999* (HMI, Berlin, 2000), p. 343.
[18] A. G. Wagh, V. C. Rakhecha, and W. Treimer, *BENSC Experimental Reports 2000* (HMI, Berlin, 2001), p. 245.
[19] H. A. Graf and J. R. Schneider, Acta Crystallogr. Sect. A **37**, 863 (1981).
[20] H. Rauch, U. Kischko, D. Petraschek, and U. Bonse, Z. Phys. B **51**, 11 (1983).
[21] W. Treimer *et al.* (to be published).